Comparison of alumina and boehmite in (APP/MPP/metal oxide) ternary systems on the thermal and fire behavior of PMMA

Blandine Friederich, Abdelghani Laachachi, Rodolphe Sonnier, Michel Ferriol, Marianne Cochez, Valerie Toniazzo, David Ruch

Comparison of alumina and boehmite in (APP/MPP/metal oxide) ternary systems on the thermal and fire behavior of PMMA

Blandine Friederich[a,b], Abdelghani Laachachi[a]*, Rodolphe Sonnier[c], Michel Ferriol[b], Marianne Cochez[b], Valérie Toniazzo[a] and David Ruch[a]

A comparison of alumina (Al_2O_3) and boehmite (AlOOH) in (ammonium polyphosphate/melamine polyphosphate/metal oxide) ternary system was performed in poly(methyl methacrylate) on thermal and fire-resistance properties. A Design of Experiments (DoE) was then done for highlighting the best formulation out of both ternary systems. Laser flash analysis and scanning electron microscopy helped to explain some of the observations made by DoE. Mechanisms in both ternary systems during degradation also were investigated and modes of action could be presented based on pyrolysis-combustion flow calorimetry, Raman spectroscopy and X-ray diffraction.

Keywords: PMMA; polyphosphate; flame retardant; metal oxide; nanocomposite

INTRODUCTION

In intumescent systems, the amount of additives necessary to reach interesting fire-resistance properties is quite high, generally leading to a worsening of the mechanical properties of the composite. In order to decrease the level of fire-retardant additives while maintaining mechanical performances, synergistic effects in intumescent systems have been developed.[1] Synergism is observed when two or more additives combined together produce a greater effect than the sum of their individual effects. Flame retardancy of poly(methyl methacrylate) (PMMA) is significantly improved by the incorporation of additives based on ammonium polyphosphate (APP). Laachachi *et al.*[2] compared two products marketed by Clariant: Exolit® AP422 and AP752 compounded with PMMA. They observed a decrease of the time to ignition (TTI) on samples containing 15% AP422 and 15% AP752. However, the most noteworthy effect was the decrease of the total heat release (THR) and of the peak of heat release rate (pHRR), especially in the case of AP752 (pHRR = 624 kW m^{-2} for PMMA, pHRR = 419 kW m^{-2} for PMMA-15%AP422, pHRR = 300 kW m^{-2} for PMMA-15%AP752). An intumescent structure was visible after cone calorimeter tests on the sample containing AP752. A comparative X-ray diffraction (XRD) study on both flame retardants disclosed that AP422 was composed mainly of pure APP and that AP752 was composed of APP and of melamine polyphosphate (MPP). MPP is less stable thermally than APP, and in the presence of heat, it quickly decompose to form ammonia which acts as a blowing agent in the intumescent system.

Metal oxides nanoparticles are known for enhancing the thermal stability of polymers. They also help to improve the fire-retardant properties. Laachachi *et al.*[2] therefore combined AP752 and metal oxides nanoparticles (alumina) in PMMA in order to benefit from the increase of thermal stability provided by the oxide nanoparticles and from the intumescent behavior of MPP and APP. The combination of these three additives led to a synergism on flame retardancy. The main goal of the present paper is to compare two metal oxides, alumina and boehmite. in (APP/MPP/metal oxide) ternary systems, when compounded in PMMA, on thermal and fire-resistance properties. The ratio of the three additives APP, MPP and metal oxide has also been optimized in order to reach the best fire-retardant properties, by means of statistical Design of Experiments (DoE) using the statistical software JMP®. The modes of action of these two ternary systems were investigated through the analysis of cone calorimeter residues and gases released during combustion.

EXPERIMENTAL

Materials

PMMA (Acrigel® DH LE, Unigel Plàsticos - M_w = 78,000 g mol^{-1} determined by means of GPC analysis) was used as the matrix. Nanometric alumina (Aeroxide® Alu C) with median particles size

* *Correspondence to: A. Laachachi, Department of Advanced Materials and Structures (AMS), Centre de Recherche Public Henri Tudor, 66 rue de Luxembourg, BP 144, L- 4002 Esch-sur-Alzette, Luxembourg.*
E-mail: abdelghani.laachachi@tudor.lu

a *B. Friederich, A. Laachachi, V. Toniazzo, D. Ruch*
Department of Advanced Materials and Structures (AMS), Centre de Recherche Public Henri Tudor, 66 rue de Luxembourg, BP 144, L-4002 Esch-sur-Alzette, Luxembourg

b *B. Friederich, M. Ferriol, M. Cochez*
LMOPS, E.A. 4423, Université Paul Verlaine Metz, Département Chimie de l'IUT de Moselle Est, 12 rue Victor Demange, BP 80105, F-57503, Saint-Avold Cedex, France

c *R. Sonnier*
Centre des Matériaux de Grande Diffusion (CMGD), Ecole des Mines d'Alès, 6 avenue de Clavières, F-30319 Alès, France

equal to 13 nm and specific surface area equal to 100 $m^2 g^{-1}$ was provided by Evonik Degussa GmbH. Boehmite (Actilox 400SM®) was given by Nabaltec (D_{50} = 350 nm). APP (Exolit® AP 422) furnished by Clariant (D_{50} = 15 μm, phosphorus content of 31–32 wt%). MPP (Melapur 200®, D_{98} = 25 μm) was given by Ciba. It contained 42–44 wt% nitrogen and 12–14 wt% phosphorus.

Nanocomposites preparation

PMMA pellets were blended with APP, MPP and metal oxides nanoparticles in a Haake PolyLab 300 cm^3 internal mixer at 225 °C and 50 rpm. The mixing time was around 7 min. The total loading of the additives was 15 wt% since PMMA loaded with 15 wt% polyphosphates showed the best results in a previous paper.[2] The compositions of the mixtures of PMMA and APP/MPP/metal oxide ternary systems are presented in Table 1. Prior to compounding, all the materials were dried in an oven at 80 °C during at least 4 h.

The extrudate was then grinded and for cone calorimeter tests, samples were pressed at 240 °C during 8 min under 55 bars with a hydraulic press from Carver.

Characterization

Thermogravimetric analysis (TGA). Thermogravimetric analyses (TGA) were performed with a STA 409 PC thermobalance from Netzsch operating under air and nitrogen flow of 100 $cm^3 min^{-1}$ in alumina crucibles (150 μL) containing about 15 mg. The runs were carried out in dynamic conditions at the constant heating rate of 10 °C min^{-1}.

Thermal diffusivity (laser flash analysis). The thermal diffusivity of PMMA and of its nanocomposites was measured from room temperature to 170 °C using a laser flash technique (Netzsch LFA 457 Microflash™) under inert and oxidative atmosphere (argon and air flows: 100 $cm^3 min^{-1}$). Thermal diffusivity was also measured on disc-shape pressed residues at 25 °C in order to follow the effect of degradation on the heat transfer of fire-retarded PMMA and to ascertain its impact on fire resistance.

Flammability (cone calorimeter). Flammability properties of PMMA-based nanocomposites were studied with a cone calorimeter device (Fire Testing Technology (FTT)). 100 × 100 × 4 mm^3 sheets of PMMA composites were exposed to a 35 kW m^{-2} radiant heat flux and forced to ignite using an electric spark. The aspiration flow was equal to 24 L s^{-1} and the results were obtained from the average values of three samples for each formulation.

Table 1. Compositions of PMMA-(APP/MPP/Al_2O_3 and AlOOH) formulations (total loading: 15 wt%)

Formulation	APP	MPP	oxide
PMMA-15%APP	1	0	0
PMMA-15%MPP	0	1	0
PMMA-15%oxide	0	0	1
PMMA-7.5%APP/7.5%MPP	1/2	1/2	0
PMMA-7.5%APP/7.5%oxide	1/2	0	1/2
PMMA-7.5%MPP/7.5%oxide	0	1/2	1/2
PMMA-5%APP/5%MPP/5%oxide	1/3	1/3	1/3

Pyrolysis-Combustion Flow Calorimetry (PCFC). The principle of PCFC relies on the separate reproduction of the solid state and gas phase processes of flaming combustion by a controlled pyrolysis of the sample in an inert gas stream, followed by a high temperature oxidation of the volatile products.[3] PCFC was performed on 1–3 mg samples using a FTT calorimeter at a heating rate of 1 °C s^{-1} up to 750 °C under nitrogen in the pyrolysis zone. The combustion zone was set at 900 °C under nitrogen/oxygen atmosphere (80/20 by volume) for a complete combustion of gases.

Design of experiments. A DoE helps to optimize a formulation in order to reach the desired specifications (named responses) with the least number of experiments. These experimental data give a mathematical formula called contour plot. Contour plots can be represented by a regression equation so that the measured and the theoretical responses are statistically equal.[4] The most commonly used model of contour plots for mixtures is the model of Scheffé,[5] but to model mixtures containing three components, it is more common to use the reduced model.[6] By using a DoE software named JMP®, the experimental data were presented into a simplex centroid design displayed in Fig. 1.[7]

A simplex centroid design was chosen because since $N = 2^q - 1$ where q is the number of components, the number of mixtures to study (N) is equal to seven.[6]

Analysis of residues. The residues were investigated by scanning electron microscopy, XRD and Raman spectroscopy. Residues morphology and chemical composition were ascertained using FEI QUANTA FEG 200 environmental scanning electron microscope. The working distance was about 10 mm, the acceleration voltage 15 kV. Wide angle XRD patterns were obtained by using a PANalytical X'Pert MPD X-ray diffractometer equipped with a copper anode emitting the radiation K_α (λ = 1.5418 Å) under a 45 kV voltage and with a 40 mA current. The diffraction tests were made with a θ/2θ diffractometer configuration. The crystalline phases were identified with the software X'Pert HighScore Plus 2.2 d from PANalytical equipped with the database ICDD PDF 4+. Raman spectroscopy study was performed at room temperature with a Horiba Jobin-Yvon LabRam spectrometer. The device has a spectral resolution of 1.4 cm^{-1}. The excitation wavelength was 514.5 nm (Ar^+ laser (Spectra Physics)). Raman spectra were measured between 9000 and 100 cm^{-1} with an acquisition time of 10 s and the final spectrum was the average of three spectra. A × 50 objective lens was used for focusing the laser beam on the sample. All spectra were recorded with a 1800 lines mm^{-1} network and a 1000 μm confocal hole. They were treated with the Labspec acquisition software.

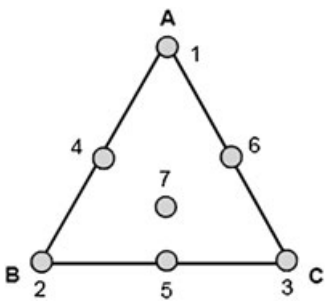

Figure 1. Simplex centroid design.

Gas analysis. Pyrolysis-gas chromatography-mass spectrometry (Py-GC-MS) analysis were performed with a CDS Pyroprobe 2000 coupled with an Agilent 6890 gas chromatograph equipped with a Optima-Wax column (high molecular weight compound of polyethylene glycol and diepoxide, 50 m length × 0.25 mm diameter 0.25 μm film thickness). The carrier gas used was helium at constant flow (1.1 mL min^{-1}). The initial sample weight was set at about 1 mg for each experiment. Flash pyrolysis was performed during 60 s at 400 °C (heating rate: 10,000 °C. s^{-1} from 20 °C to 400 °C).

RESULTS AND DISCUSSION

Thermal properties

TGA was performed upon heating from room temperature to 900 °C under air and under nitrogen atmosphere. The results are presented in Fig. 2.

Since TGA curves showed a single step of thermal degradation, the PMMA is either anionically polymerized or stabilized. Table 2 presents the starting degradation temperature at which the degradation starts ($T_{10\%}$: temperature at 10% weight loss) and the temperature at half weight loss ($T_{50\%}$) of PMMA, PMMA-APP/MPP/Al_2O_3 and PMMA-APP/MPP/AlOOH systems.

According to Fig. 2, all curves are shifted to higher temperatures compared to PMMA in both air and nitrogen. However, all samples were less thermally stable under air than under nitrogen, as shown by the starting degradation temperature ($T_{10\%}$) and the temperature at half weight loss ($T_{50\%}$) values. PMMA degraded in one step showing that the polymer was polymerized by an anionic way.

When added at 15 wt% into PMMA, the metal oxides nanoparticles delayed $T_{10\%}$ by 18 °C under air and by 10 °C under nitrogen compared to pristine PMMA ($T_{10\%}$ = 302 °C under air, $T_{10\%}$ = 337 °C under nitrogen) (Table 2). They also improved the thermal stability at half weight loss by 11–15 °C under air and by 9 °C under nitrogen, always towards pure PMMA ($T_{10\%}$ = 331 °C under air, $T_{10\%}$ = 368 °C under nitrogen). This improvement of the thermal stability by metal oxides is mainly due to the restriction of mobility polymer chain as discussed in previous papers.[2,5]

The shape of TGA curves exhibits a modification of the degradation mechanism in the presence of APP (at 15 wt%), especially under oxidative atmosphere (Fig. 2b). By comparison with PMMA, that formulation shows no improvement at $T_{50\%}$ despite an enhancement at the beginning of the decomposition. According to Camino *et al.*,[8] APP decomposes into three steps. Below 260 °C, a part of APP transforms into more stable APP (II), with release of ammonia and water[9] (reaction).

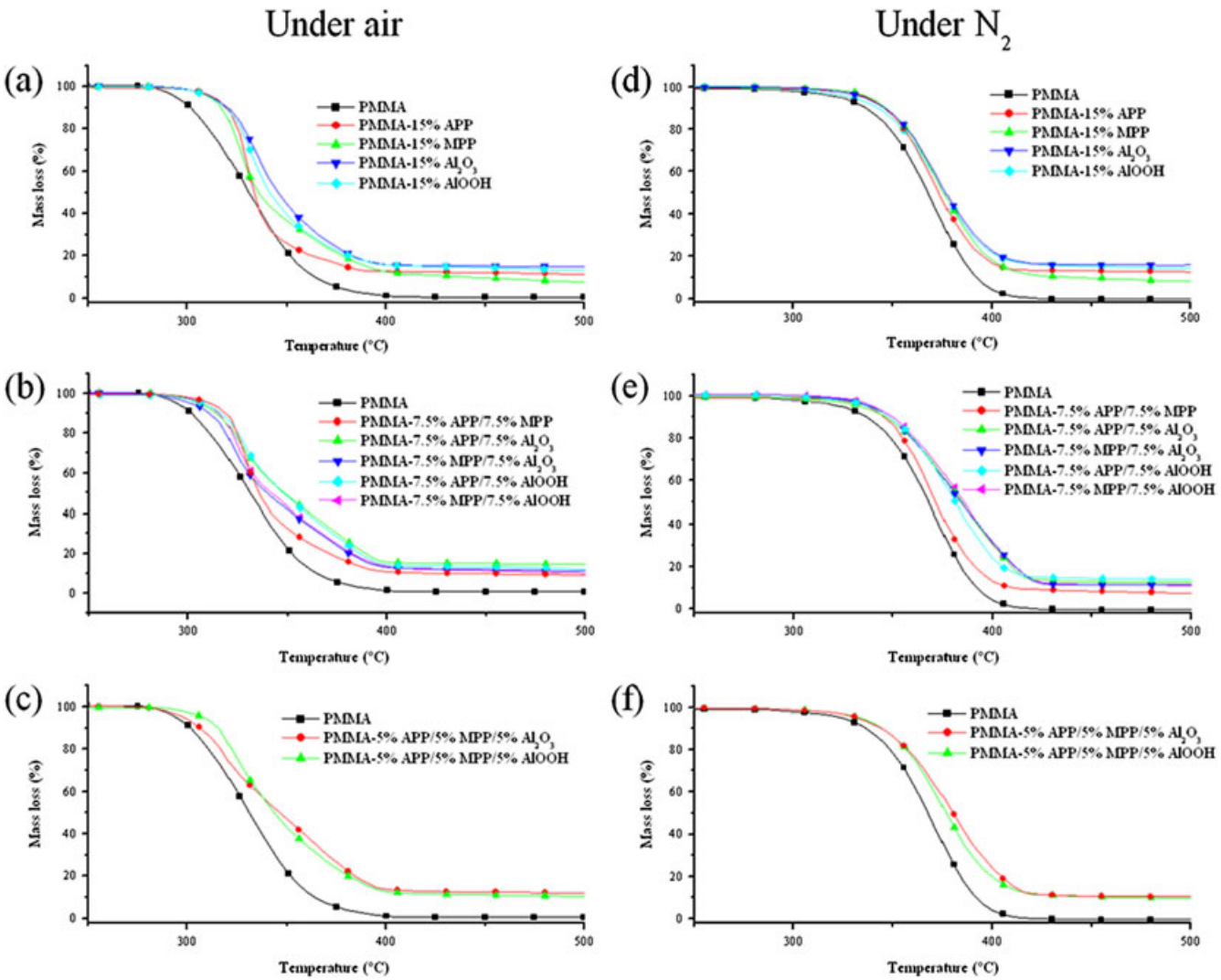

Figure 2. TGA curves of PMMA, PMMA-APP/MPP/Al_2O_3 and PMMA-APP/MPP/AlOOH systems under air (a, b, c) and under nitrogen (d, e, f).

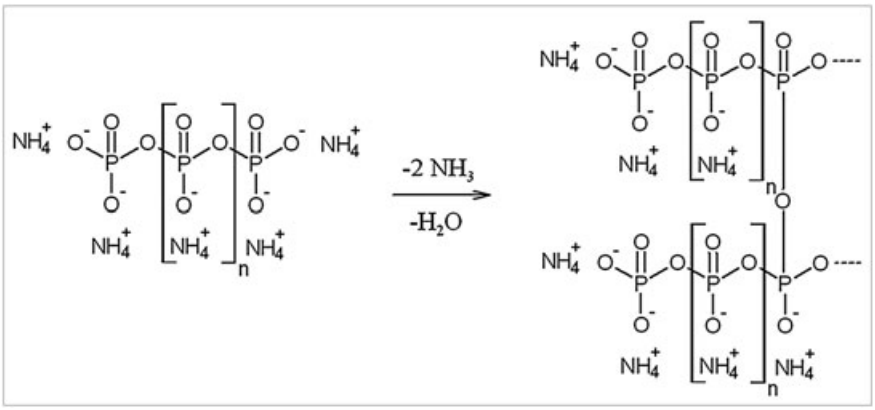

At 260–370 °C, ultraphosphate residues decompose giving salts of ammonium phosphate, ammonia, water and polyphosphoric acid. At higher temperatures, polyphosphoric acid degrades into volatile phosphorated fragments which condense at room temperature. The same authors showed that there is no reaction between PMMA and the degradation products of the first reaction. Therefore, the absence of improvement concerning the thermal stability of PMMA-15%APP compared to PMMA is mainly due to reactions between PMMA and polyphosphoric acid leading to an anhydride and methanol through cyclization. This reaction and the depolymerization process of PMMA are competitive.[9] The substitution of a part of APP with MPP leads to a weak enhancement of the thermal stability under air and nitrogen (Fig. 2b, e), because MPP like APP decomposes into phosphoric acid. Besides the char that then developed through the reaction between polyphosphoric acid and the polymer protects the material from the heat, flames and oxygen and inhibits the release of free radical gases.

On the contrary, the substitution of a part of APP or MPP with a metal oxide leads to an improvement of the thermal stability. Indeed, a shift of up to 15 °C was noticed for the formulations containing metal oxides, compared to PMMA-15%APP and PMMA-15%MPP (Table 2). The metal oxides nanoparticles therefore reinforced the barrier effect by restraining the mobility of polymer chains. The increase of the viscosity reduced the release of gases degradation out of the sample. The combination of APP, MPP and Al_2O_3 or AlOOH (Fig. 2c, f) also leads to a significant enhancement of the stability (up to 16 °C), but PMMA-5%APP/5%MPP/5%Al_2O_3 shows a catalytic effect at the beginning of degradation in the presence of oxygen.

To conclude, formulations containing metal oxides, especially boehmite, APP and MPP, exhibit the best results under both atmospheres.

Flammability

Cone calorimeter

The fire-retardancy properties of PMMA-APP/MPP/Al_2O_3 and PMMA-APP/MPP/AlOOH systems have been studied by cone calorimetry under an incident flux of 35 kW m^{-2}. During this test, several parameters can be measured: TTI, time of flame out (TOF), pHRR, THR, smoke emission (TCOR) together with the mass loss of the sample. Table 3 shows the main data obtained on both ternary systems (5% standard deviation).

In Table 3, the combustion time corresponds to the difference between TOF and TTI, the pHRR decrease is the percent of decrease of the pHRR compared to PMMA and the fire

Table 2. Temperatures at 10% and 50% weight loss ($T_{10\%}$ and $T_{50\%}$) for PMMA-APP/MPP/Al_2O_3 and PMMA-APP/MPP/AlOOH systems under air and nitrogen (heating rate: 10 °C min^{-1})

	Under air		Under N_2	
	$T_{10\%}$ (°C)	$T_{50\%}$ (°C)	$T_{10\%}$ (°C)	$T_{50\%}$ (°C)
PMMA	302	331	337	368
PMMA-15%APP	320	333	346	373
PMMA-15%MPP	318	336	347	376
PMMA-15%Al_2O_3	320	346	346	377
PMMA-15%AlOOH	321	342	343	376
PMMA-7.5%APP/7.5%MPP	319	335	346	371
PMMA-7.5%APP/7.5% Al_2O_3	315	348	346	384
PMMA-7.5%APP/7.5%AlOOH	311	348	349	381
PMMA-7.5%MPP/7.5% Al_2O_3	317	339	348	384
PMMA-7.5%MPP/7.5%AlOOH	316	341	350	385
PMMA-5%APP/5%MPP/5%Al_2O_3	307	347	344	380
PMMA-5%APP/5%MPP/5%AlOOH	316	344	345	377

Table 3. Cone calorimeter data of PMMA-APP/MPP/Al_2O_3 and PMMA-APP/MPP/AlOOH systems

	TTI(s)	TOF(s)	Combustion time (s)	pHRR ($kW.m^{-2}$)	pHRR decrease (%)	Fire Performance Index ($kW^{-1}.m^2.s$)	THR ($MJ.m^{-2}$)	Final residues (%)	TCOR ($g.kg^{-1}$)
PMMA	62	339	337	533	/	0.116	117	0	7
PMMA-15%APP	*63*	*560*	*497*	*345*	*35*	*0.183*	*100*	*12*	*10*
PMMA-15%MPP	67	675	608	260	51	0.258	99	6	21
PMMA-15%Al_2O_3	88	500	412	350	34	0.251	81	14	14
PMMA-15%AlOOH	67	501	434	351	34	0.191	104	14	14
PMMA-7.5%APP/7.5%MPP	58	710	652	255	52	0.227	103	10	7
PMMA-7.5%APP/7.5%Al_2O_3	58	643	595	309	42	0.155	80	17	19
PMMA-7.5%APP/7.5%AlOOH	65	836	771	236	56	0.275	92	14	14
PMMA-7.5%MPP/7.5%Al_2O_3	61	693	642	315	41	0.162	89	14	15
PMMA-7.5%MPP/7.5%AlOOH	72	900	828	251	53	0.287	98	12	11
PMMA-5%APP/5%MPP/5%Al_2O_3	58	613	565	332	38	0.145	88	12	16
PMMA-5%APP/5%MPP/5%AlOOH	71	939	868	226	58	0.314	95	8	8

performance index (FPI) is the ratio of TTI and pHRR. The data presented in Table 3 showed that the THR decreases for all blends in comparison with PMMA. Moreover, the ignition was delayed for PMMA compounded with metal oxides. PMMA-7.5%MPP/7.5%AlOOH and PMMA-5%APP/5%MPP/5%AlOOH exhibited the longest combustion time with a delay in the time of ignition compared to PMMA. The lowest pHRR were obtained for PMMA-15%MPP, PMMA-7.5%APP/7.5%MPP and for PMMA containing AlOOH combined with APP and/or MPP.

Figure 3 displays the evolution of HRR and the mass loss as a function of time for both ternary systems under a heat flow of 35 kW m^{-2}.

MPP in PMMA leads to a significant reduction of pHRR (51% compared to PMMA) as shown in Table 3 and Fig. 3a. It is reported in the literature[10] that MPP decomposes endothermically above 350 °C, acting as a heat sink to cool down the polymer. The phosphoric acid released reacts with the polymer to form a char which protects the polymer substrate from heat, flames and oxygen and inhibits the release of free radical gases into the oxygen phase. Simultaneously, nitrogen species (ammonia) released from the degradation of melamine swells the char to further protect the polymer. Ammonia also dilutes radicals and flammable gases, slowing down the combustion.[10] The mode of action of MPP explains the improvement of pHRR observed in our study in PMMA. By comparison, MPP appears more efficient than APP; this is due to the fact that APP releases less ammonia which leads to the swelling of the upper layer of the sample.

Combining phosphorus-based fire retardants with alumina or boehmite leads to the decrease of the pHRR, but the formulations containing boehmite have much better results as shown in Fig. 3b, c. That improvement is also visible on the mass loss rate (Fig. 3e, f) which is lower for boehmite-based formulations. The slowdown of the mass loss rate originating from the modification of the kinetics of polymer degradation is related to the increase of the time of combustion for PMMA. The combination of MPP with boehmite leads to a pHRR reduction of 53%, whereas 15 wt% boehmite in PMMA only leads to 34% pHRR decrease. It appears that a synergy effect takes place when MPP and AlOOH are combined. Synergism is also detected when APP, MPP and AlOOH are combined together (pHRR decrease of 58 % with 226 kW m^{-2}). Hence, PMMA-5%APP/5%MPP/5% AlOOH is the best formulation for fire-resistance properties and has the highest FPI, ratio of TTI and pHRR. The most notable synergy effect occurred between AlOOH and APP: 15 % APP only lead to a decrease of 35% of the pHRR and 15% AlOOH to 34%, but their association led to a pHRR decrease of 56%. That formulation also exhibited one of the highest FPI.

The DoE presented in Fig. 4 and performed for pHRR and TTI confirmed that statement since the best sample is located near the region having the lowest pHRR and the highest TTI.

DoE is a helpful way to organize experimental tests to obtain the maximum information with the minimum number of tests and formulations.[11] On Fig. 4, it is observable that the progressive substitution of metal oxide nanoparticles with MPP caused a pHRR decrease. High pHRR performances for a ceramized sample (PMMA-5%APP/5%MPP/5%AlOOH) could be reached, and they were close to the performances of a purely intumescent sample (PMMA-15%MPP), but without the swelling effect.

For PMMA-(APP/MPP/Al_2O_3), the progressive substitution of alumina with phosphorus-based FR leads to a decrease in TTI until reaching a value close to that of PMMA (Fig. 5). The substitution of alumina with MPP leads to the decrease in the pHRR whereas the substitution with APP brings about no change in pHRR. Thus, the DoE presented in Fig. 5 confirms the fact that the alumina-based ternary system is not an optimal formulation since the zone where the pHRR is low and the one where the TTI is high are not superimposed.

MPP has a prevailing effect on the reduction of TTI, because it systematically results in the fall of TTI even for formulations containing alumina having the highest TTI value (88 s). A decrease of TTI is often pointed out for intumescent systems; it comes from the upsurge of the polymer degradation by the additives.[12]

Figure 6 displays photographs of residues of PMMA-APP/MPP/Al_2O_3 and PMMA-APP/MPP/AlOOH after cone calorimeter tests.

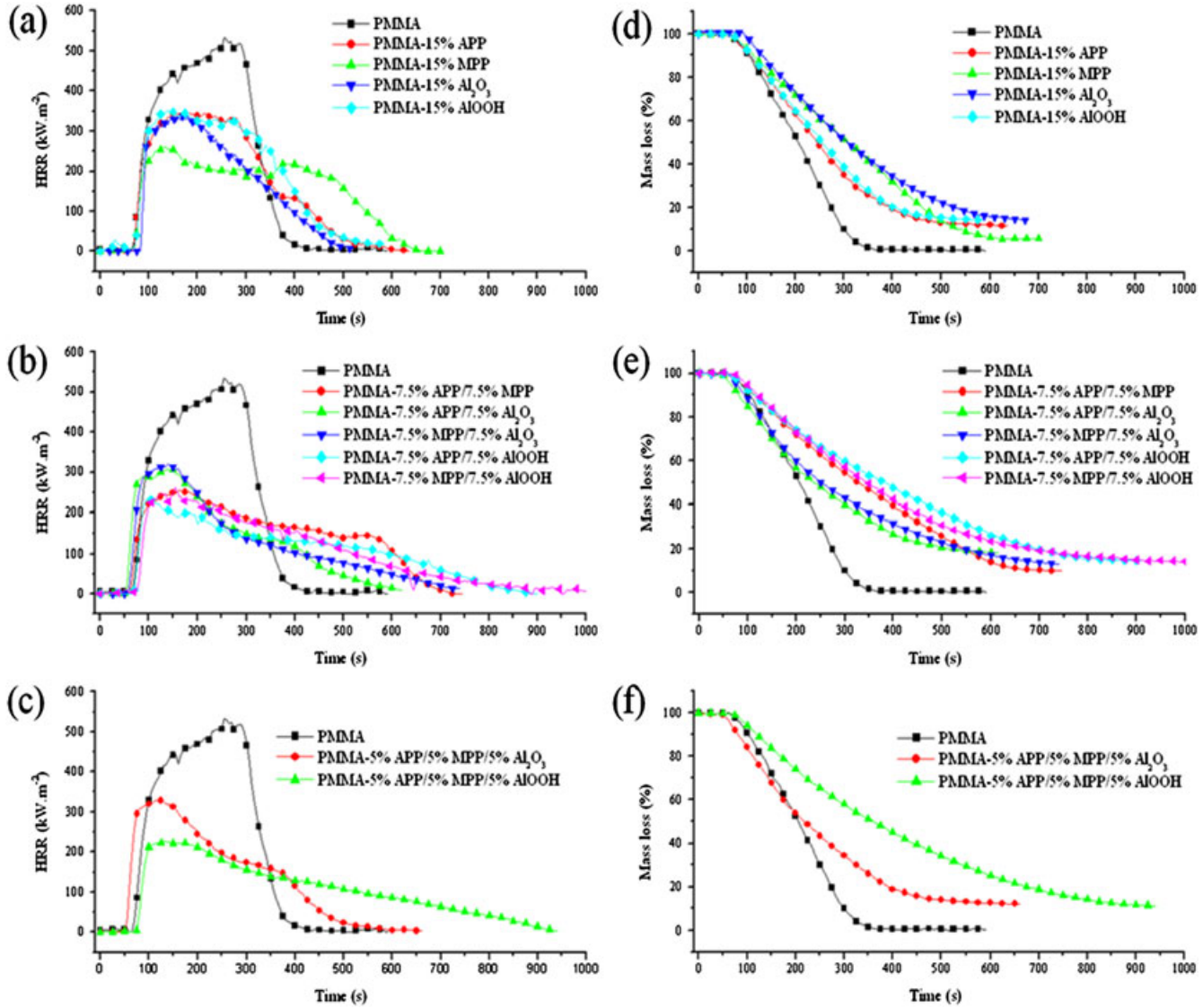

Figure 3. pHRR (a, b, c) and mass loss (d, e, f) for PMMA-APP/MPP/Al_2O_3 and PMMA-APP/MPP/AlOOH systems measured by cone calorimetry (heat flux: 35 kW m^{-2}).

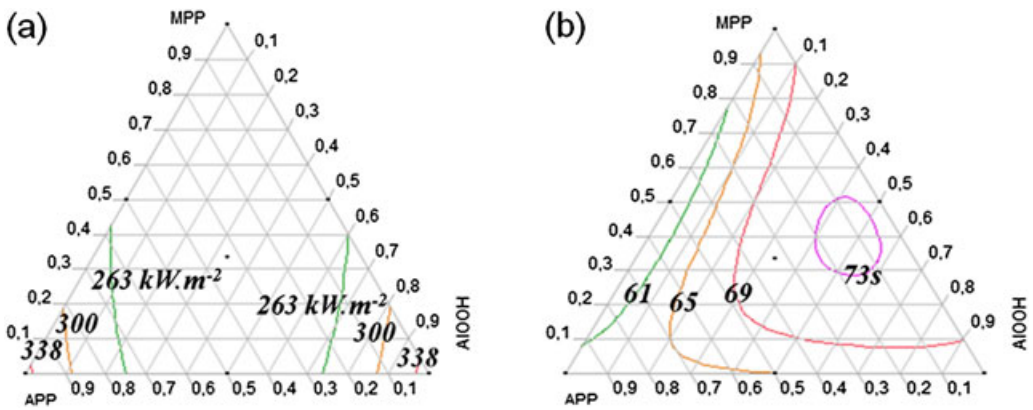

Figure 4. Variations of pHRR (a) and TTI (b) within PMMA-APP/MPP/AlOOH.

It is observable on Fig. 6 that PMMA-15%MPP is the sample exhibiting the most important intumescent structure due to the release of ammonia, protecting the material from the flames, heat and oxygen.[13] Since the residues of the ternary system containing alumina were not continuous, this could be one of the reasons why these formulations were not that good concerning fire resistance.

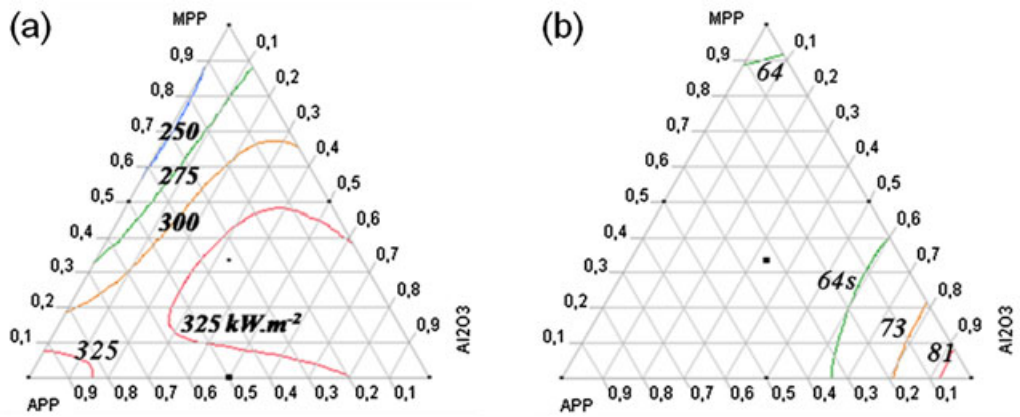

Figure 5. Variations of pHRR (a) and TTI (b) within PMMA-APP/MPP/Al_2O_3.

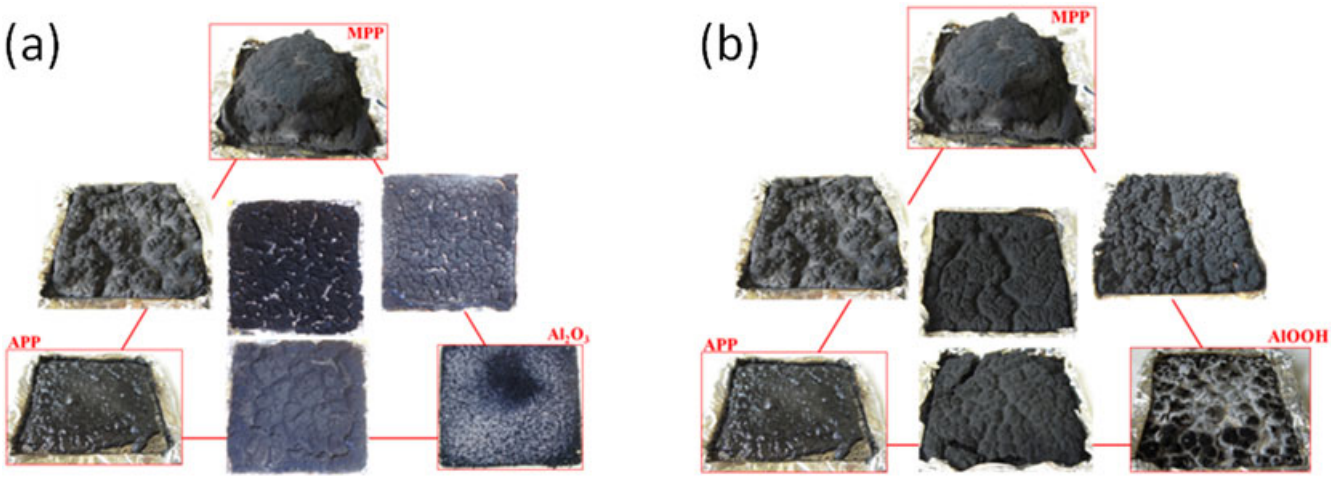

Figure 6. Cone calorimeter residues of (a) PMMA-APP/MPP/Al_2O_3 and (b) PMMA-APP/MPP/AlOOH ternary systems.

Table 4. Pyrolysis Combustion Flow Calorimeter pHRR and pHRR decrease for PMMA-APP/MPP/Al_2O_3 and PMMA-APP/MPP/AlOOH systems compared to cone calorimeter data

	PCFC		Cone calorimeter	
	pHRR (kW m^{-2})	pHRR decrease (%)	pHRR (W g^{-1})	pHRR decrease (%)
PMMA	402	/	533	/
PMMA-15%APP	371	8	345	35
PMMA-15%MPP	323	20	260	51
PMMA-15%Al_2O_3	309	23	350	34
PMMA-15%AlOOH	295	27	351	34
PMMA-7.5%APP/7.5%MPP	361	10	255	52
PMMA-7.5%APP/7.5%Al_2O_3	294	27	309	42
PMMA-7.5%APP/7.5%AlOOH	321	20	236	56
PMMA-7.5%MPP/7.5%Al_2O_3	311	23	315	41
PMMA-7.5%MPP/7.5%AlOOH	293	27	251	53
PMMA-5%APP/5%MPP/5%Al_2O_3	304	24	332	38
PMMA-5%APP/5%MPP/5%AlOOH	312	22	226	58

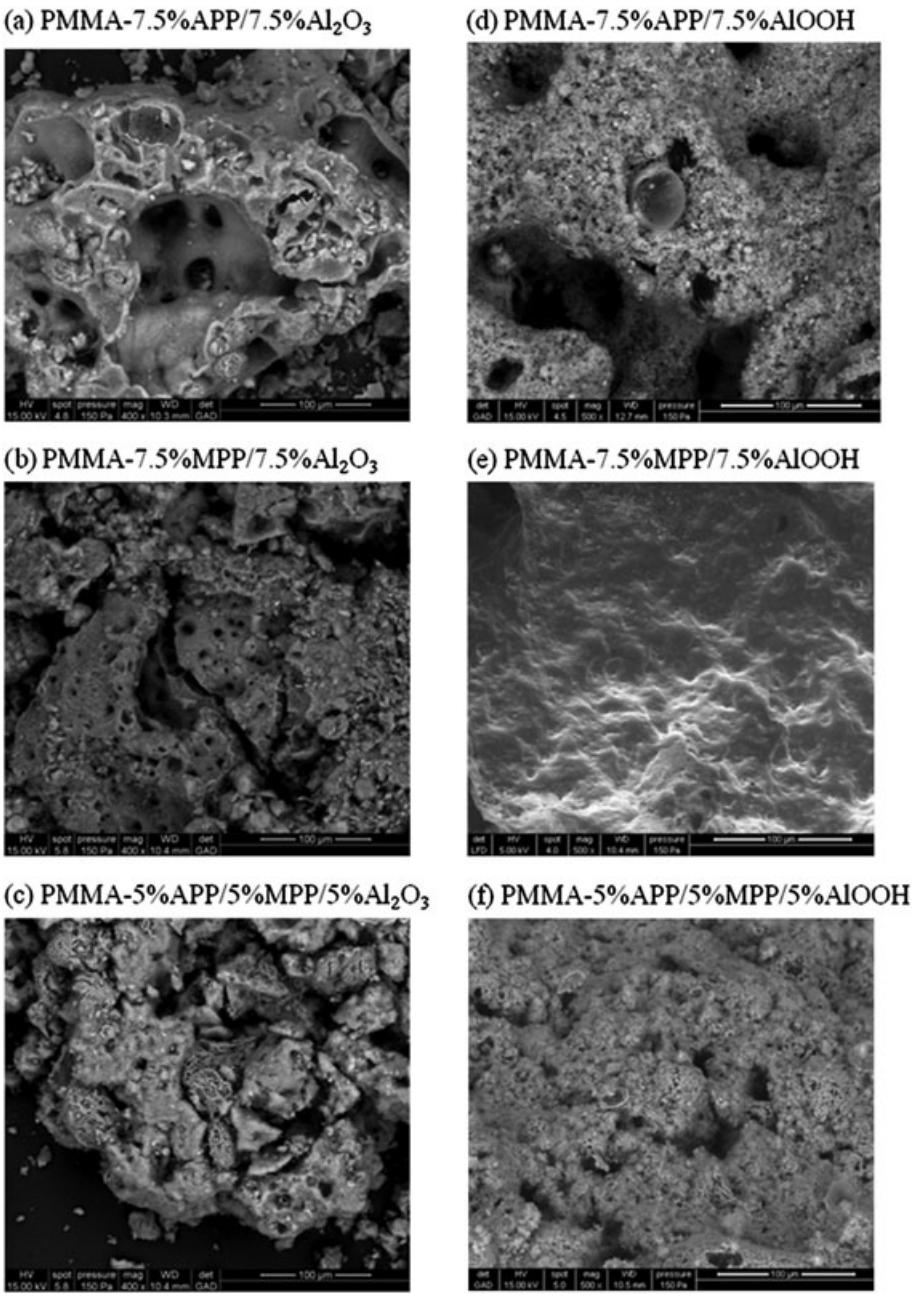

Figure 7. Comparison between residues' micrographs of PMMA-APP/MPP/Al_2O_3 (a, b, c) and of PMMA-APP/MPP/AlOOH (d, e, f) composites.

Pyrolysis Combustion Flow Calorimeter (PCFC)

Since fire retardants can act either by a chemical effect, a physical action or by both of them, the complementarity between PCFC and cone calorimetry allows determining in which way the fire retardants have a prevailing action. Indeed, there is a complete combustion of gases released after pyrolysis in PCFC taking only into account processes occurring via chemical mechanisms, whereas cone calorimetry focuses on processes occurring by chemical and physical mechanisms. Table 3 gives the pHRR values measured by PCFC compared to cone calorimeter measurements.

According to Table 4, in PMMA-15% APP, PMMA-15% MPP and PMMA-7.5%APP/7.5%MPP, the pHRR decrease is much more important in cone calorimetry than in PCFC, signifying that the fire protection is mainly due to a barrier effect. On the contrary, alumina and boehmite alone in PMMA shows similar pHRR decreases in PCFC and in cone calorimetry (around 30%), meaning that the barrier protection is not the main effect on fire resistance in these formulations. The decrease of the pHRR can be due to the endothermic reaction of AlOOH or to the polymer chain mobility of metal oxides nanoparticles. The release of water was confirmed by Py-GC-MS. When boehmite is combined with phosphorus-based fire retardants, its mode of action occurs more by a physical way (mainly barrier effect) whereas when alumina is associated with APP and/or MPP, mechanisms of fire resistance mainly occurs by a chemical way.

The mechanisms of decomposition of the different formulations have then been investigated through the analyses of residues obtained after cone calorimetry and of the emitted gases during pyrolysis.

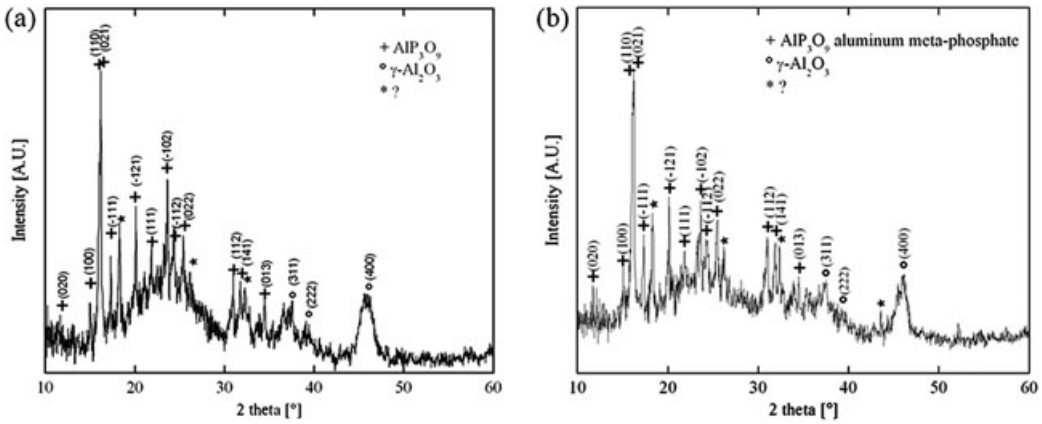

Figure 8. XRD spectra of residues of (a) PMMA-7.5%APP/7.5% Al_2O_3 and (b) PMMA-7.5%APP/7.5% AlOOH.

DISCUSSION

The chemical structure and morphology of the condensed phase (residues) were investigated by Raman spectroscopy, XRD and SEM. These techniques gave information on the compounds formed during burning and those remaining. The gas phase was analyzed by Py-GC-MS in order to know which gases were released during pyrolysis. The combination of these methods could help to get a complete scheme of degradation of the fire-retarded PMMA and to explain some phenomena observed on thermal degradation and fire-resistance properties.

The only visual observation of residues in Fig. 6 is not sufficient to conclude on formulations. A deeper insight through SEM micrographs is given in Fig. 7.

In this figure, it is observable that boehmite-based residues are more compact and present less holes than alumina-based one. These holes appear during the degradation and cause the release of gases and hinder the efficiency of the barrier effect. The lack of efficiency of the physical protection for all alumina-based formulations is confirmed by PCFC (Table 4), because their major action can be attributed to a chemical action (respectively 68%, 64%, 56% and 63% for PMMA-15%Al_2O_3, PMMA-7,5%APP/7,5%Al_2O_3, PMMA-7,5%MPP/7,5%Al_2O_3 and PMMA-5%APP/5%MPP/5%Al_2O_3).[14] This constitutes one element for explaining why better flammability properties are observed in the case of AlOOH.

Moreover, according to PCFC tests, boehmite alone acts by 79% by a chemical action through a catalytic effect of the surface of the particles leading to a char formation upon burning. When compounded with APP, these formulations (PMMA-7.5%APP/7.5%AlOOH and PMMA-5%APP/5%MPP/5% AlOOH) have a prevailing action through a physical protection with a proportion of, respectively, 64% and 62%. This statement is in agreement with the micrographs presented in Fig. 7 which shows more compact residues compared to alumina-based one. XRD shows reactivity between APP and AlOOH through the formation of aluminum meta-phosphate (AlP_3O_9) (Fig. 8). The formation of AlP_3O_9 was detected by XRD in alumina-based formulations (Fig. 8a). All crystalline boehmite is transformed into alumina since no boehmite could be detected by XRD on residues, without excluding the possibility of the presence of amorphous boehmite in residues. The resulting spectrum is presented in Fig. 8b.

According to Moorlag *et al.*,[15] products from the reaction between alumina and phosphoric acid (H_3PO_4, degradation product of APP), in the temperature range of 100–500 °C, are: aluminum orthophosphate ($AlPO_4$) and/or aluminum metaphosphate (AlP_3O_9) via other phosphate-based phases. High-phosphate-content phases are exclusively favored by high-phosphate conditions (Al:P $\leq$ 0.5). Alumina was also detected after combustion due to reaction 1:

$$2AlOOH \rightarrow Al_2O_3 + H_2O \quad (1)$$

This release of water was confirmed by Py-GC-MS for PMMA-15% AlOOH. All the gases evolved during burning were analyzed by Py-GC-MS for completing the proposed mechanism. In order to compare the variation of the pyrolysates compositions as a function of the proportion of APP, MPP and metal oxides nanoparticles, the total ion current (TIC) chromatograms were normalized to unity of mass for each formulation. Since MMA monomer is always produced in high quantities saturating the mass detector, the ions currents corresponding to the following molecular ions: m/z = 18 (water), m/z = 28 (carbon monoxide), m/z = 32 (methanol) and m/z = 86 (methacrylic acid or MAA) were extracted from TIC chromatograms in order to avoid any interference. After integration, the evolution of the peak areas of these three ions was compared for each formulation.

Py-GC-MS tests also showed that the good flammability properties of the APP/MPP/AlOOH system are not only due to the barrier effect observed by SEM (formation of few holes), but also to the release of water, through the endothermic reaction, which dilutes flammable gases and radicals in the gas phase. The amount of methanol evolved in the case of boehmite is twice than for titanium dioxide in Ref. 16 and steadily increased with the boehmite loading (Fig. 9e), whereas the quantity of MAA (Fig. 9f) is much lower than in the literature[16] while regularly increasing with the boehmite loading (0, 5, 7.5 and 15 wt%).

In that boehmite-based ternary system, the release of methanol is probably due to the reaction between the ester groups of PMMA and the hydroxyls groups present on the surface of boehmite particles according to the reaction scheme in Ref. 16 for titanium dioxide. A low production of MAA means that its production is competing with another reaction such as depolymerization. The overall mechanism for that system is presented in Fig. 10.

In the alumina-based ternary system, the release of methanol and of MAA does not increase steadily with the alumina loading, because there is a "bump" around 5–7.5 wt% polyphosphates. According to Camino *et al.*,[8] the degradation of PMMA in the

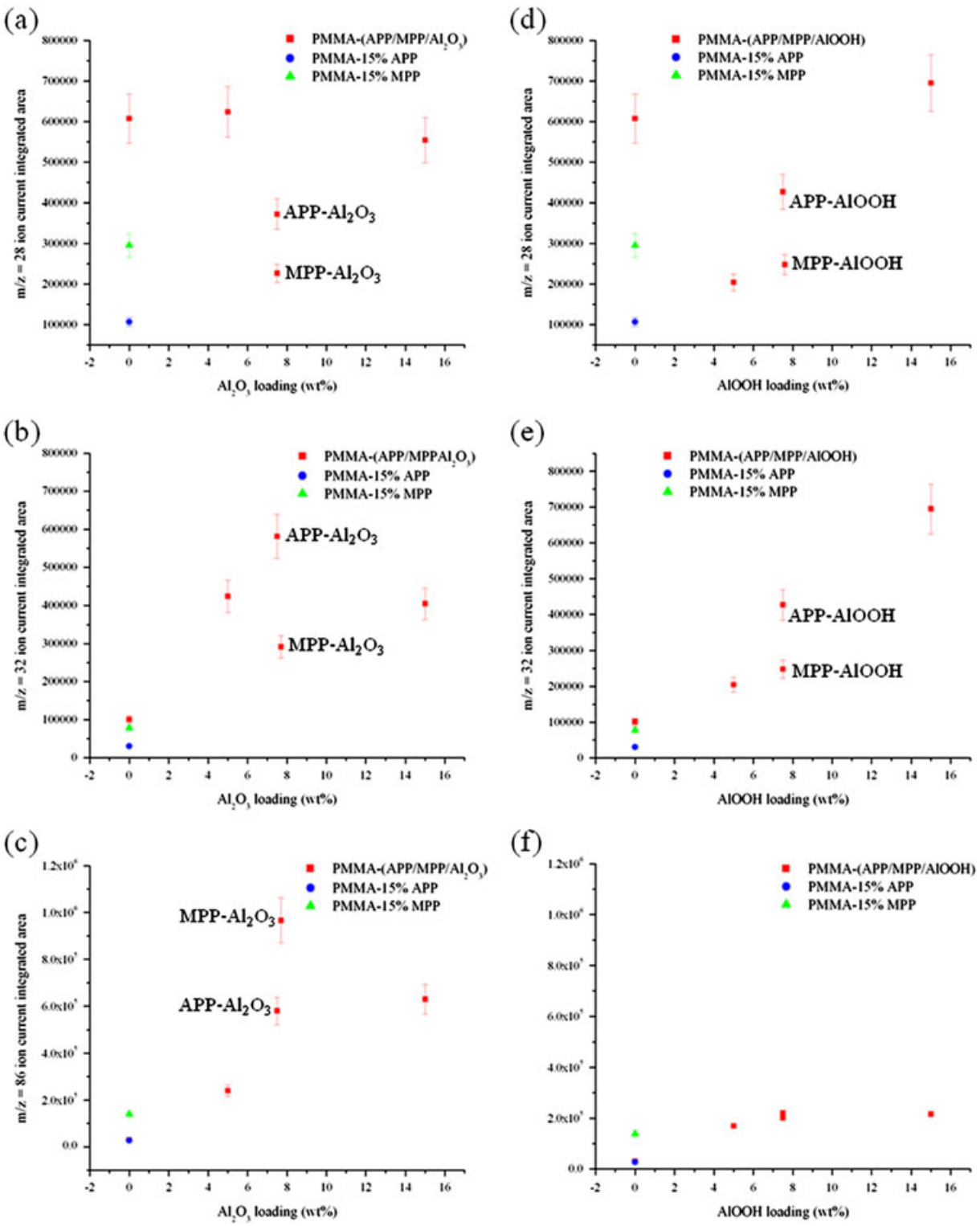

Figure 9. Ion current integrated areas of m/z = 28 (carbon monoxide), m/z = 32 (methanol) and m/z = 86 (methacrylic acid) for (a–c) PMMA-(APP/MPP/Al_2O_3) and (d-f) PMMA-(APP/MPP/AlOOH) systems.

presence of polyphosphoric acid (a reaction product of APP degradation) leads to the cyclization of MMA to give anhydride units accompanied by the production of methanol. Therefore, the methanol released through cyclization added to the methanol amount evolves during the reaction between –OH functions of the surface of alumina nanoparticles and ester groups of PMMA.[16] This can explain the higher level of methanol observed around 5–7.5 wt% polyphosphates. The high amount of MAA in the same region could come from rearrangement reactions during the cyclization. The cyclization reaction, which takes place parallel to the reaction between –OH groups and esters, is presented in Fig. 11.

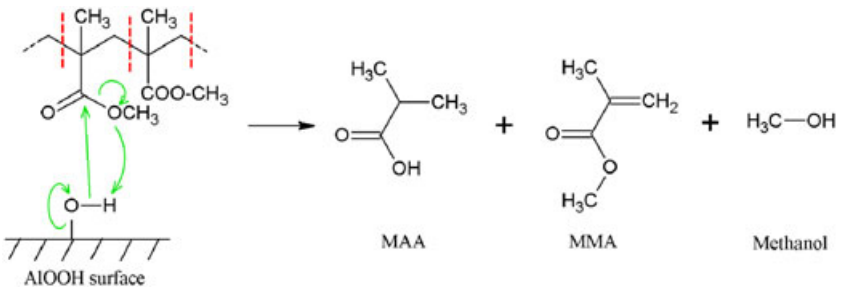

Figure 10. Degradation mechanism of PMMA-AlOOH.

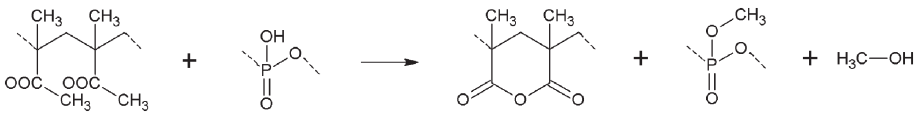

Figure 11. Reaction of cylization between PMMA and polyphosphoric acid in PMMA-(APP/MPP/Al_2O_3) ternary system.

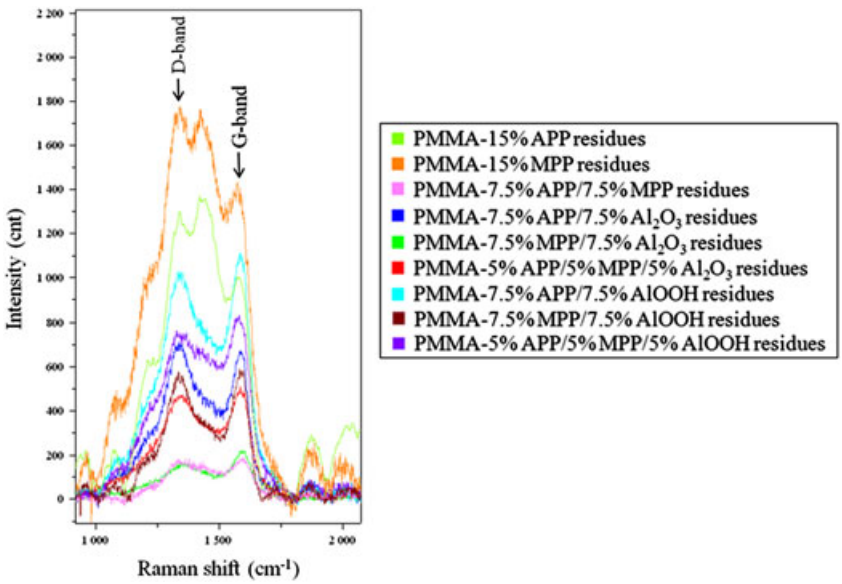

Figure 12. Raman spectroscopy spectra of PMMA-(APP/MPP/Al_2O_3) and PMMA-(APP/MPP/AlOOH) residues.

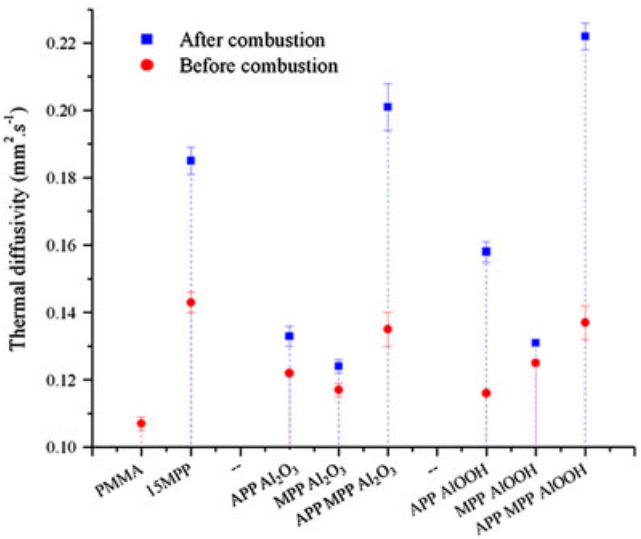

Figure 13. Thermal diffusivity measurement of PMMA-(APP/MPP/Al_2O_3) and PMMA-(APP/MPP/AlOOH) after degradation.

Therefore in the boehmite-based ternary system, the cyclization reaction takes over the formation of MAA. The system also releases a low amount of CO (Fig. 9d), meaning that the combustion was nearly complete. On the contrary, the alumina-based system presents an incomplete combustion (Fig. 9a and Table 3), because the level of CO evolved is higher than that in the other ternary system; this gives to the system the possibility to form a barrier to the oxygen despite the presence of holes which were observed by SEM (Fig. 7).

The visual observation of samples obtained after flammability tests showed the presence of a carbonaceous layer (Fig. 6). Its existence was ascertained by Raman spectroscopy, it allowed to detect the formation of aromatic hydrocarbons in the residues of all formulations containing at least one additive, through the presence of D- and G-bands at respectively 1350 and 1580 cm^{-1} (Fig. 12).

The D-band represents the disordered graphite such as clusters of hexagonal rings. It is associated to the A_{1g} vibrational mode and is usually called the "defect band". The G-band is related to the ordered graphite which originates from the

ordered hexagonal rings consisting of conducting sp^2-bonded carbon, and it corresponds to the E_{2g} vibrational mode, i.e. C–C vibrations in the aromatic layers.[17–19]

XRD, Raman spectroscopy and SEM-EDS have proved not only a change in the structure of the samples upon combustion, but also a chemical reactivity between the additives. Moreover, a change of the thermal diffusivity of the samples was also noticed after combustion. This has been measured by laser flash analysis (LFA). The thermal diffusivity of PMMA-(APP/MPP/Al_2O_3) and PMMA-(APP/MPP/AlOOH) ternary systems was measured before and after combustion to show the effect of a modification of composition upon combustion on the heat transfer. The thermal diffusivity was measured on cone calorimeter pressed residues using LFA. Figure 13 presents these measurements at 25 °C after combustion.

The incorporation of additives into PMMA increases the thermal diffusivity as evidenced in a previous paper.[20] For all formulations, the thermal diffusivity of the material increases after burning; it means that the burned material dissipates the heat better than unburned one leading to a slowdown of the thermal degradation. The thermal diffusivity is an intrinsic value of the material since the samples were compressed for practical reasons. According to Kashiwagi *et al*.,[21] the residual layer has also an insulation effect due to the foamy structure of the residues protecting the material from the heat. In our case, the residual layer has therefore a double impact on heat transfer: an insulation effect due to its foamy structure and a heat dissipation effect coming from the material's thermal properties themselves. However, both effects led to the protection of the sample upon degradation.

Three residues (PMMA-15%MPP, PMMA-5%APP/5%MPP/5% Al_2O_3 and PMMA-5%APP/5%MPP/5%AlOOH) differ from others by their higher thermal diffusivity which is respectively: $0.185 \pm 0.004\,mm^2\,s^{-1}$, $0.201 \pm 0.007\,mm^2\,s^{-1}$ and $0.222 \pm 0.004\,mm^2\,s^{-1}$ (Fig. 13). PMMA-5%APP/5%MPP/5%AlOOH is the best formulation concerning the heat dissipation. It has been observed by Raman spectroscopy (Fig. 12) that the presence of APP and/or MPP in PMMA leads to the formation of aromatic hydrocarbons during combustion. Aromatic hydrocarbon-based materials are known for having high thermal diffusivity values. Xie *et al*.[22] showed that the thermal diffusivity of carbon nanotubes could reach $4.6\,cm^2\,s^{-1}$. This statement could explain why residues of samples containing 7.5 wt% of polyphosphates before combustion exhibit thermal diffusivity values between 0.12 and $0.16\,mm^2\,s^{-1}$ and residues of samples containing 10 to 15 wt% of polyphosphates before combustion dissipate the heat better with thermal diffusivities higher than $0.18\,mm^2\,s^{-1}$. It is noteworthy to mention that in the present study, the thermal diffusivity of residues was measured on pressed samples. It means that when taking into account the porosity of the residues could change the ranking of performances of the samples.

CONCLUSION

Boehmite-based ternary system exhibits better flammability properties than the system containing alumina. More precisely, the best synergy effect on the pHRR is observed for PMMA-7.5%APP/7.5% AlOOH. PMMA-5%APP/5%MPP/5%AlOOH presents the best fire resistance properties with the highest pHRR decrease (58% compared to PMMA) and the highest FPI (0.314). This is confirmed by the DoE. Therefore, for that ceramized sample, close pHRR performances to an intumescent sample can be reached. The residues of that formulation exhibit the highest thermal diffusivity value; this can be explained by the formation of aromatic hydrocarbons which has a high heat dissipation capacity. It has also been shown that AlOOH reacted with PMMA giving MAA and methanol. A competition between that reaction and PMMA depolymerization was proposed for explaining the low MAA release.

Acknowledgements

The authors gratefully acknowledge the financial support of the Fonds National de la Recherche from Luxembourg. Evonik-Degussa, Nabaltec, Clariant and Ciba are acknowledged for giving respectively alumina, boehmite, APP and MPP.

REFERENCES

[1] S. Duquesne, S. Bourbigot, R. Delobel, Synergism in intumescent systems – a review, In: *Advances in the flame retardancy of polymeric materials, Current perspectives*, presented at FRPM'05 (Ed.: B. Schartel), Books on Demand GmbH, Norderstedt, Germany, **2005**, 15–34.
[2] A. Laachachi, M. Cochez, E. Leroy, P. Gaudon, M. Ferriol, J. M. Lopez-Cuesta, *Polym. Adv. Technol.* **2006**, *17*, 327.
[3] R. E. Lyon, R. N. Walters, *J. Anal. Appl. Pyrol.* **2004**, *71*, 27.
[4] H. Dvir, *Compos. Sci. Technol.* **2003**, *63*, 1865.
[5] H. Scheffé, *J. Roy. Stat. Soc. B Met.* **1963**, *25*, 235.
[6] NIST, Engineering Statistics Handbook. Available from: www.itl.nist.gov/div898/handbook/eda/eda.htm [accessed 15 March **2011**].
[7] J. Goupy, *Revue MODULAD* **2006**, *34*, 74.
[8] G. Camino, N. Grassie, I. C. McNeill, *J. Polym. Sci. Pol. Chem.* **1978**, *16*, 95.
[9] G. Camino, L. Costa, L. Trossarelli, *Polym. Degrad. Stabil.* **1985**, *12*, 203.
[10] Ciba-BASF, Flame retardants: Melapur 200. http://worldaccount.basf.com/wa/EU~en_GB/Catalog/PlasticAdditivesEU/pi/BASF/subindustry/prod_class_flm_ret [accessed 15 March **2011**].
[11] J. Goupy, *Techniques de l'Ingénieur* **2000**, *R 275*, 1.
[12] S. Bourbigot, S. Duquesne, *Intumescence-based fire retardants*, In: *Fire Retardancy of Polymeric Materials* (Eds.: C. A. Wilkie, A. B. Morgan), CRC Press, Boca Raton, **2010**, 129–162.
[13] S. Bourbigot, S. Duquesne, Intumescence and Nanocomposites: a Novel Route for Flame-Retarding Polymeric Materials, In: *Flame Retardant Polymer Nanocomposites* (Eds.: A. B. Morgan, C. A. Wilkie), John Wiley & Sons, Hoboken, **2006**, 131–162.
[14] F. Laoutid, R. Sonnier, D. Francois, L. Bonnaud, N. Cinausero, J. M. Lopez-Cuesta, P. Dubois, *Polym. Advan. Technol.* **2010**, DOI: 10.1002/pat.1661.
[15] C. Moorlag, Q. Yang, T. Troczynski, J. Bretherton, C. Fyfe, *J. Am. Ceram. Soc.* **2004**, *87*, 2064.
[16] A. Laachachi, M. Ferriol, M. Cochez, D. Ruch, J. M. Lopez-Cuesta, *Polym. Degrad. Stabil.* **2008**, *93*, 1131.
[17] S. Bourbigot, M. Le Bras, R. Delobel, *Carbon* **1993**, *31*, 1219.
[18] L. Song, K. Wu, Y. Wang, Z. Wang, Y. Hu, *J. Macromol. Sci. A* **2009**, *46*, 290.
[19] J. Robertson, *Mater. Sci. Eng.* **2002**, *R. 37*, 129.
[20] B. Friederich, A. Laachachi, M. Ferriol, D. Ruch, M. Cochez, V. Toniazzo, *Polym. Degrad. Stabil.* **2010**, *95*, 1183.
[21] T. Kashiwagi, F. Du, K. I. Winey, K. M. Groth, J. R. Shields, S. P. Bellayer, H. Kim, J. F. Douglas, *Polymer* **2005**, *46*, 471.
[22] H. Xie, A. Cai, X. Wang, *Phys. Lett. A* **2007**, *369*, 120.